

# Using a 3D-Printed Waveguide Filter with Ridge Resonators as a Dielectric Permittivity Sensor

Francesco Romano, Nicolò Delmonte<sup>1</sup>, Luca Perregrini, Maurizio Bozzi

<sup>#</sup>University of Pavia, Department of Electrical, Computer and Biomedical Engineering, Pavia, Italy

<sup>1</sup>nicolo.delmonte01@universitadipavia.it

**Abstract**—This paper presents the use of a waveguide filter with ridge resonators that exhibits transmission zeros to implement a dielectric permittivity sensor. Thanks to its geometry, the electric field is intense under the ridge resonators, where the dielectric slab to be characterized is located. The operation principle is based on the evaluation of the frequency shift of transmission zeros, and exhibits high sensitivity and tolerance to vertical positioning errors. The designed sensor operates around the frequency of 10 GHz. The manufacturing process is based on the 3D printing with plastic material and the subsequent metallization. A set of commercial dielectric laminates have been adopted to validate the performance of the sensor.

**Keywords**—Additive manufacturing, dielectric permittivity, sensor, waveguide.

## I. INTRODUCTION

Dielectric materials play a central role in the realm of microwave engineering. The applications of such materials are extremely broad, ranging from acting as substrates for planar components and circuits, to loading resonant cavities to produce compact filters and multiplexers. The fundamental characteristic of these materials is the dielectric permittivity  $\epsilon_r$ . Any difference between the nominal value of the dielectric permittivity used in the design of a component and the actual value of the physically employed material will result in a change in the performance of the implemented device; this can be particularly detrimental in the case of resonant devices like narrowband filters, which have to take into account the effect of this uncertainty using tuning mechanisms.

In this context, the ability to characterize the dielectric permittivity of a material in a fast and accurate way plays an important role. To this end, many different sensor structures have been studied and proposed. Many of them are based on the measurement of the shift of the frequency of a resonator when loaded with the material under test [1]. This method is flexible, and can be applied to various material, including solid slabs [2,3] and fluids [4,5].

Multiple resonators can be coupled together in order to obtain filters with transmission zeroes. The presence of a dielectric material near the resonators will affect the frequency of the zeroes. In this work, a sensor based on this effect is presented. The component is implemented in rectangular waveguide, and the resonators employed are the slanted ridge iris [6,7]: this topology allows to obtain transmission zeroes in a particularly compact layout. Moreover, the resonant mode of slanted irises has its electric field concentrated in a small gap, making it sensitive to even small amounts of material with low dielectric permittivity. The component is fabricated using

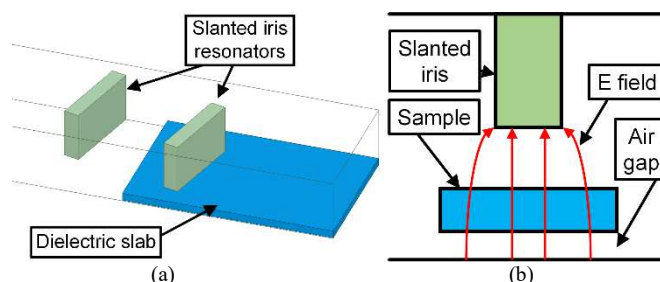


Fig. 1. (a) Topology of the 3D printed slanted iris resonator dielectric sensor; (b) Detail of the electric field distribution below the slanted iris.

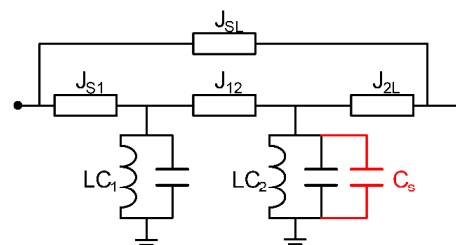


Fig. 2. Equivalent circuit of the printed slanted resonator dielectric sensor. The presence of the dielectric slab acts on the additional capacitance  $C_3$  of one of the resonators.

additive manufacturing; this technology has been recently under intense research for the creation of waveguides and other 3D structures with the aim of adding design flexibility, reducing the cost and increasing the component integration [8,9].

## II. OPERATION PRINCIPLES

The sensor is based on the design of one of the bandpass filters presented in [7]. That component employs slanted ridge resonators: this topology allows to obtain transmission zeroes in a simple inline filter configuration due to indirect signal coupling paths. The topology of the component can be perturbed in an asymmetrical way by placing a dielectric slab below one of the slanted irises, as shown in Fig. 1a. The presence of the dielectric material acts as a capacitive loading for its resonant mode (Fig. 2), lowering its resonance frequency. This shift also affects the position of all the transmission zeroes. The additional loading capacitance depends both on the thickness and the dielectric permittivity of the slab. This means that by inserting a sample with known thickness inside the device, it is possible to retrieve the value of  $\epsilon_r$  by measuring the shift in the frequency of the transmission zeroes compared to when the component is unloaded.

In addition, the small gap below the iris tends to have a capacitive behavior even when unloaded. The electrical field

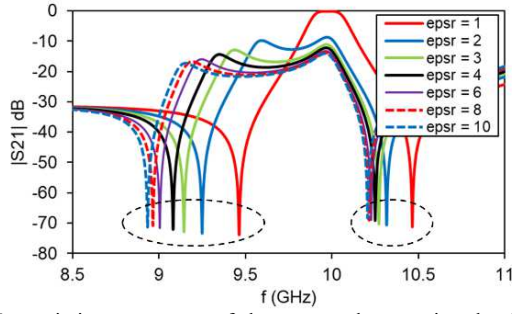


Fig. 3. Transmission parameters of the sensor when varying the dielectric permittivity of the slab. Results obtained with slab thickness of 30 mils.

tends to be vertical and concentrated under the iris (Fig. 1b): this makes the sensor more resilient to the presence of air gaps between the dielectric slab and the bottom of the waveguide, making the setup more robust to sample positioning errors compared to other traditional methods. An example of the behavior of the component is shown in the simulation of Fig. 3, where the dielectric permittivity of a slab with thickness 30 mil is swept between 1 and 10. Compared to the reflection zeroes, the transmission zeroes remain sharp and well defined even when the dielectric loading degrades the matching of the device. The position of the transmission zeroes results more sensitive with lower dielectric permittivity values. The frequency shift of the transmission zero compared to the unloaded case can be interpolated by the equation:

$$\Delta f_z = a \cdot \epsilon_r^b + c \quad (1)$$

where the value of coefficients  $a$ ,  $b$  and  $c$  depend on the size of the slab, and the transmission zero which is being considered. The coefficients can be extracted from the results of electromagnetic simulations. The values computed for the proposed sensor are shown in Table 1. In the measurement phase, the frequency shift is obtained and the dielectric permittivity of the slab is retrieved by inverting the previous equation:

$$\epsilon_r = \sqrt[b]{\frac{\Delta f_z - c}{a}}. \quad (2)$$

### III. PROTOTYPE FABRICATION AND MEASUREMENT

The physical dimensions of the component, based on the layout of Fig. 4, are the following:  $a_w = 22.86$  mm,  $b_w = 10.16$  mm,  $l_w = 7$  cm,  $l = 14$  mm,  $w = 2.55$  mm,  $s = 17.75$  mm,  $t = 1.99$  mm,  $g = 2$  mm, and  $\theta = 76^\circ$ . This results in a frequency response with two transmission zeroes, spaced 1 GHz and centered around 10 GHz.

Table 1. Coefficients of the model for dielectric permittivity retrieval (frequencies in MHz)

Coefficient		Substrate thickness		
		10 mil	20 mil	30 mil
Lower transmission zero	$a$	-127.7	-366.2	-829.1
	$b$	-0.83	-0.61	-0.44
	$c$	127.5	366	827.6
Upper transmission zero	$a$	-99.3	-197.5	-280.4
	$b$	-0.99	-0.99	-1.06
	$c$	99.2	197.8	280.9

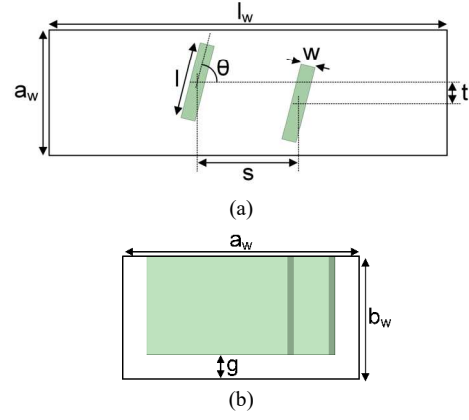


Fig. 4. Physical dimensions of the 3D printed slanted resonator dielectric sensor.

The component has been fabricated via additive manufacturing. The first step in the fabrication process is the creation of a plastic support, which replicates the shape and size of the component. This was achieved using the Stratasys Connex 3 printer. In order to connect the device to the measurement setup, standard WR90 flanges are also added at both ends of the component. The next step consists in an initial metallization of the internal walls of the device, which was done by applying a layer of silver-based conductive paint. This step requires access to the inner side of the component: for this reason, the plastic support is split in two parts which are treated independently. After that, the parts undergo galvanic electroplating to cover them with a layer of highly conducting copper, to improve electromagnetic performance. Finally, the parts are assembled together and held using a set of screws to ensure the electrical contact. The result of the process is shown in Fig. 5.

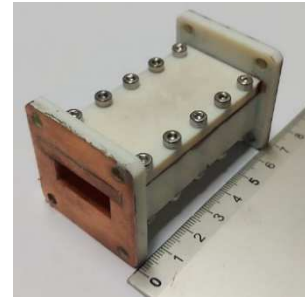


Fig. 5. Prototype of the 3D printed slanted resonator dielectric sensor.

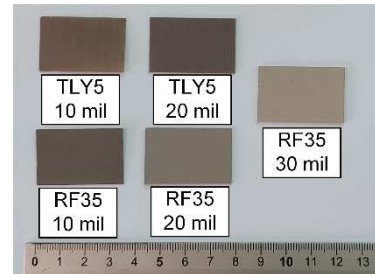


Fig. 6. Picture of the dielectric samples used to validate the 3D-printed slanted resonator dielectric sensor.

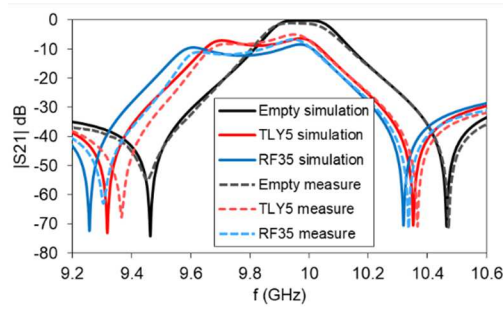


Fig. 7. Comparison between measurements and simulations of the 3D printed slanted resonator dielectric sensor, with sample thickness 20 mil.

A set of samples had to be performed in order to validate the performance of the sensor. They have been obtained by machining some slabs of commercial RF substrates with different thickness and permittivity: Taconic TLY5 ( $\epsilon_r = 2.2$ ,  $\tan\delta = 0.0009$ ) with thickness 10 mil and 20 mil and Taconic RF35 ( $\epsilon_r = 3.5$ ,  $\tan\delta = 0.0018$ ) with thickness 10, 20, and 30 mil.

Since the dielectric substrates are provided with upper and lower copper cladding, the metal cover has been completely removed using chemical etching. A picture of the samples is shown in Fig. 6. The size of the samples is 35 x 22.8 mm: the dimensions have been chosen to be exactly half of the length of the device, to make it easier to position and align the slab when inserting it from the edge of the structure. Measurements are performed with and without the dielectric sample, to determine the frequency shift of the transmission zeroes. Fig. 7 shows an example of such a measurement, with sample thickness of 20 mil.

A plot of the models used to extrapolate the permittivity, derived from equation (2), is shown in Fig. 8. In the same figures, the measured frequency shift of each sample is also plotted along its nominal dielectric permittivity: the offset between the point and the model curve represents the measurement error.

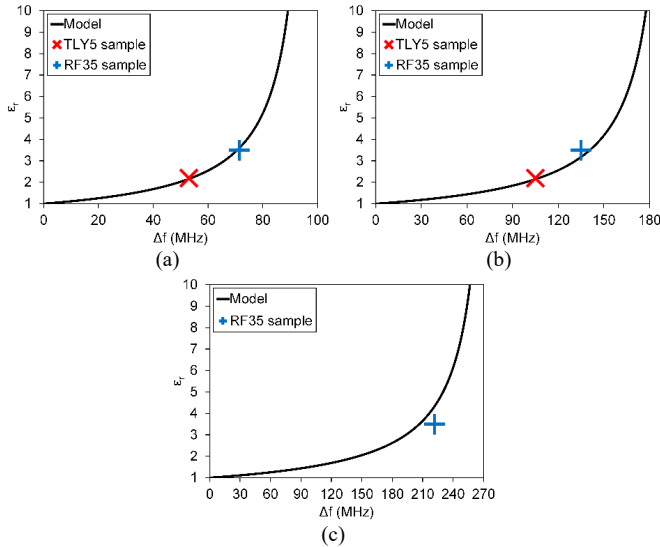


Fig. 8. Retrieval of the dielectric permittivity using the model of equation (2) using the upper transmission zero frequency with different dielectric sample thicknesses: (a) 10 mil; (b) 20 mil; (c) 30 mil.

Table 2. Results of the measurements of known dielectric samples

Dielectric material	Nominal $\epsilon_r$	Sample thickness	Retrieved $\epsilon_r$	Error
TLY5	2.2	10 mil	2.16	-2%
		20 mil	2.14	-2.6%
RF35	3.5	10 mil	3.6	+3%
		20 mil	3.18	-9.2%
		30 mil	3.73	+6.5%

As the thickness of the sample becomes higher, the frequency shift increases, along as the sensitivity of the sensor. Table 2 presents the summary of the retrieved values for all the samples. It can be seen that the sensor is more accurate with lower slab thicknesses. For thickness 10 mil, the measured values are within the manufacturer tolerance.

#### IV. CONCLUSION

This work presented a dielectric sensor that employs a waveguide filter based on slanted iris resonators, which exhibits a passband and two transmission zeros. The sensing mechanism is based on the frequency shift of the transmission zeros. The slanted irises make the component resistant to vertical positioning errors of the dielectric sample (air gaps). To further improve the precision of the measurement, a shallow groove may be placed on the lower side of the structure to reduce the horizontal positioning error of the sample. This can be done exploiting the flexibility of the additive manufacturing process.

#### REFERENCES

- [1] A. W. Kraszewski and S. O. Nelson, "Observations on resonant cavity perturbation by dielectric objects," *IEEE Transactions on Microwave Theory and Techniques*, vol. 40, no. 1, pp. 151-155, Jan. 1992.
- [2] N. K. Tiwari, A. K. Jha, S. P. Singh, Z. Akhter, P. K. Varshney and M. J. Akhtar, "Generalized Multimode SIW Cavity-Based Sensor for Retrieval of Complex Permittivity of Materials," *IEEE Transactions on Microwave Theory and Techniques*, vol. 66, no. 6, pp. 3063-3072, June 2018.
- [3] A. Ebrahimi, J. Scott and K. Ghorbani, "Dual-Mode Resonator for Simultaneous Permittivity and Thickness Measurement of Dielectrics," *IEEE Sensors Journal*, vol. 20, no. 1, pp. 185-192, 1 Jan. 1, 2020.
- [4] G. Gennarelli, S. Romeo, M. R. Scarfi and F. Soldovieri, "A Microwave Resonant Sensor for Concentration Measurements of Liquid Solutions," *IEEE Sensors Journal*, vol. 13, no. 5, pp. 1857-1864, May 2013.
- [5] M. A. H. Ansari, A. K. Jha, Z. Akhter and M. J. Akhtar, "Multi-Band RF Planar Sensor Using Complementary Split Ring Resonator for Testing of Dielectric Materials," *IEEE Sensors Journal*, vol. 18, no. 16, pp. 6596-6606, 15 Aug. 15, 2018.
- [6] S. Bastioli, L. Marcaccioli and R. Sorrentino, "Waveguide Pseudoelliptic Filters Using Slant and Transverse Rectangular Ridge Resonators," *IEEE Transactions on Microwave Theory and Techniques*, vol. 56, no. 12, pp. 3129-3136, Dec. 2008.
- [7] F. Romano, N. Delmonte, C. Tomassoni, L. Perregrini and M. Bozzi, "3D-Printed Compact Waveguide Filters Based on Slanted Ridge Resonators," *2022 IEEE/MTT-S International Microwave Symposium - IMS 2022*, 2022, pp. 96-99.
- [8] H. Xin and M. Liang, "3-D-Printed Microwave and THz Devices Using Polymer Jetting Techniques," *Proceedings of the IEEE*, vol. 105, no. 4, pp. 737-755, April 2017.
- [9] C. Tomassoni, O. A. Peverini, G. Venzoni, G. Addamo, F. Paonessa and G. Virone, "3D Printing of Microwave and Millimeter-Wave Filters: Additive Manufacturing Technologies Applied in the Development of High-Performance Filters with Novel Topologies," *IEEE Microwave Magazine*, vol. 21, no. 6, pp. 24-45, June 2020.